Answers to Referee 2

April 15, 2022

1 Detailed comments

CGMs Table 1: the selection of GCMs used should be justified. This could be through reference to model performance literature for key parameters, a specific evaluation process or perhaps simply availability of required variables for the analysis (though I note the variables used are available for all CMIP5 models).

The choice of the CGMs was driven by the availability of the variables of interest in the Copernicus Climate data store (CDS) in the representative concentration pathways used in the exercise (RCP 2.6, 4.5 and 8.5 W/m2) in both single and pressure levels monthly data in the same ensemble (r1i1p1). We also aimed at having multiple regions represented.

Shifted extraction Section 2.2: the MSLP from ERA-5 is sampled 500 km from the centre of the cyclone. Is the same done for the other variables? Since the data are sampled from monthly means,it's possible the sampled values may not accurately represent the conditions at the time of TC passage (especially relevant for variables with sharp gradients such as SST).

We retrieve both pressure (MSLP) and humidity (RH) to define P^{env} and RH^{env} (Holland, 1997) away from the center because TC maximum potential intensity (MPI) - through thermodynamic efficiency and moist entropy - arise from the deviations from the normal conditions. We acknowledge that monthly averaging may indeed "smooth" values so that the data may not represent the conditions at the time of cyclone passage. Therefore, using monthly means, this translation is mainly made for reasons of theoretical coherence. In future studies, this model will be applied with higher temporal resolution and performing this translation would be more important. In the present version of our paper, because the CMIP5 projections of the sea-level temperature were only available at monthly frequency in the CDS, we chose to perform the exercise using monthly data to illustrate our approach. In addition the monthly sampled data allowed us to build a statistically significant description of the MPI in the historical period. The possibility of improving the model using high frequency data will be emphasized in the revised version of the manuscript.

Common metrics Section 3.2: Given the literature of TC track generation methods, comparison with common metrics is encouraged. Specifically, as landfall is critical to reliable performance of a damage model, it would be helpful to present a comparison of the observed and simulated landfall rates (see for example Arthur (2021), Hall and Jewson (2007), and Lee et al. (2016)). This would strengthen the quality of the track generation results significantly.

In the revised version we will compute landfall rates and compare them to relevant results from the literature.

WPR Eq 3 - note that most best track data used wind pressure relations (WPRs) to determine Pc. Typically the work flow involves determining the Dvorak T number, converting this to a sustained wind speed, followed by regionally-specific WPR to determine Pc. The conversion back to wind speed from reported Pc using a single WPR will introduce errors, as an array of WPRs are used to operationally estimate Pc, not only between basins but within basins as well (J. Courtney, 2009; J. Courtney & Burton, 2018; J. B. Courtney et al., 2021; Harper, 2002).

We acknowledge that the use of a single WPR (in line with Bloemendaal et al. (2020)) introduces errors. Figure 1, presents the WPR estimated from historical track data in different basins, and shows that when using a single WPR the winds are likely to be underestimated in the East Pacific and north Indian basin.In the revised version we shall estimate WPR parameters separately for each basin, include the references provided by the reviewer and update Figure 9 consequently.

Figure 1: WPR per basin

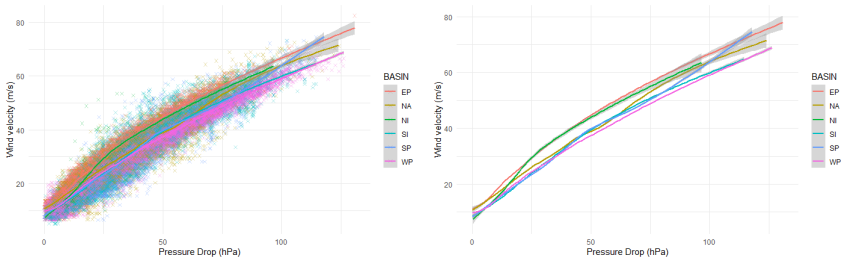

Uses of MDP Eq 10 describes the dominant control on the maximum intensity of TCs (maximum pressure drop - MDP). This is tied only to SSTs. The model uses maximum potential intensity (MPI) to control the depression dynamics (i.e. intensification rates). The formulation of MPI is directly applicable to the problem of estimating the maximum intensity, accounting for factors beyond SST alone that control maximum intensity. This suggests using SST as the only predictor of the MDP is deficient.

Indeed, we already acknowledge that the SST alone in not a good predictor of whether individual TC will intensify. Therefore, we use the thermodynamic definition in the cyclone dynamics specification. On the other hand, we still define a "MPD" taking the maximum observed pressure drop for a given SST across all events in each basin. You are right to point out that this appears to be inconsistent. However, we use this maximum depression (MPD) estimated over the historical period for a given sea surface temperature only to cap the depressions in the simulations, to avoid generating events intensifying beyond past observations and make the simulated tracks more realistic. This is a limitation of our approach, however this is relatively common in "statistical" models. Alternatively, we could make the maximum depression depend on the four variables of interest, however, this would make estimation more difficult and reduce the significance of this statistic.

In the revised version we will compare our definition with an alternative definition of the MPD, using the thermodynamic definition used for the MPI, and substituting extreme values of temperature and humidity.

Dynamics factor Further,Chen et al. (2021) suggest rapid intensification is dependent on dynamical (e.g. upper divergence and wind shear) as well as thermodynamical factors. While the difference between Pc and MPI is a factor in predicting rapid intensification, and the dynamical factors are probably accounted for by the random innovation (Eq. 12), these other dynamical factors should be acknowledged.

Indeed, the components explaining the noise term in the pressure dynamics should be better identified, and we will acknowledge them in the next version of the manuscript. However, in the context of our exercise we had to focus on explanatory factors that are available in the CMIP5 simulations which reduced our scope to thermodynamical factors.

CDF-t Apply CDF-t to model variables, then evaluate MPI - I suggest comparing quantiles of ERA5 MPI against the bias corrected CMIP MPI values to demonstrate the effect of bias correction. Q-Q plots would be an effective way to do this. One risk with this approach is that correcting individual variables may lead to unrealistic combinations when evaluating MPI - e.g. extremely low tropopause temperatures in combination with very high SSTs that lead to unrealistic lapse rates and therefore unrealistically large MPI. Two solutions present themselves: 1) apply the bias correction methods to calculated MPI or (2) consider the joint distributions of variables when evaluating the bias corrections.

This is a very relevant point. Indeed, individual variables entering the MPI computation may be strongly correlated as shown in Figure 2. In the revised version we will follow the reviewer's suggestion and apply bias correction directly to calculated MPI.

SST distributions The distributions of SST presented in Figure 16 do not appear representative of SSTs sampled in the vicinity of TCs, and is inconsistent

Figure 2: Correlation levels (global) of modeled variables affecting the MPI with their reference values in ERA5

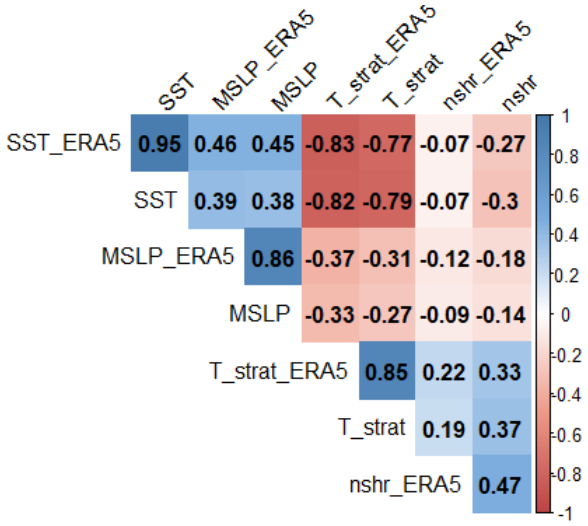

with the distribution shown in Figure 10. SSTs of 26C (299K) are typically considered a lower bound for TC formation (Gray, 1979), but median values from the ERA5 are well below that - for example based on Figure 16 the median SST for the South Pacific basin along synthetic tracks is 290-292K, for the Western Pacific 295K. Only the N Indian basin has a median SST near 300K. This suggests that the synthetic tracks are traversing areas not typically covered by TCs, or occurring at the wrong time of year for the respective basin leading to the unusual SST distribution.

The bias-correction module is indeed fitted on a larger range of climate conditions. By definition, for the genesis of the cyclones, the time of year and location are in line with historical cyclone data. However, in the bias-correction module, the synthetic tracks are generated without climate constraints, i.e. cyclones are allowed to drift relatively far away from their genesis location (in the limits of their initial basin), and therefore can cover conditions which do not lead to the formation of tropical cyclones. At this stage, these tracks are not to be considered as 'TCs tracks' but as 'candidate' tracks. In the following stage, TC tracks will be generated from candidate tracks by filtering those ones where meteorologiocal conditions for cyclone formation are satisfied.

Discussion Completely absent is any discussion on TC rates in the projections. Comprehensive literature reviews and expert elicitations indicate a global decline in TC frequency (albeit with generally low-medium confidence) (Knutson et al., 2020). Changes in TC rates will have a significant impact on the annualised losses. This is an important component that should be addressed. In parallel, there is no discussion on changes in track behaviour. Observed trends

in TC translation speed (Kossin, 2018) and poleward migration of maximum intensity (Kossin et al., 2014) should be considered in projections of TC activity. This has profound implications for TC-related risk in key marginal areas (Bruyère et al., 2019) where vulnerabilities are high, but present-day frequency of TCs is low.

These two comments will be included in the conclusion of the revised version of our paper as they reflect important limitations of our exercise. Indeed, we kept the genesis rates constant for each basin. The number of cyclones each year are drawn from Poisson distribution. It is possible to reduce the intensity parameter in the projections, and to introduce cyclones in regions where the present-day frequency is low, however, in this study, we focused on the changes in thermodynamic potentials. Moreover, as our approach is a statistical one, we had to focus on areas where relationships could be extrapolated from historical data. We will add a comment to account for this possible improvement.

Shared Socioeconomic Pathways Section 5.2: Consideration of SSPs in determining the effects on damage is novel, but the explanation is very limited. Given growth of exposure is constrained in existing high exposure regions, regional growth may not be in areas exposed to TC impacts.

In the revised version, we will provide more explanations about the shared-socioeconomic pathways used to project exposure. Indeed, we did not consider that areas subject to cyclones would face additional economic growth constraints in our projections. Historically, high exposure regions were not particularly constrained in terms of growth (e.g. the East Coast of the United States of America can be considered as a high exposure region as well as most regions in South Korea, Japan, Australia). In addition, climate change increases tropical cyclone intensity allowing them to reach regions where current TC impacts are low.

Description projection exposure The description of the implementation of projections of local physical asset value dynamics is very limited, but probably the most novel part of the connected modelling system. There should be a more substantial discussion on how the SSP definitions are used to modify asset values.

To estimate future exposures along the cyclone track in each scenario, we use the downscaled estimation for the exposed wealth (Eberenz et al., 2020) and the coefficients representing the change between the current state and the future scenario in the framework of the shared-socioeconmic pathways (Jones & O'Neill, 2020; O'Neill et al., 2017; O'Neill et al., 2014).

The local physical exposure at the coordinates (x, y) at time t in a region j in scenario k is defined as follows:

$$\Phi(x, y, j, k, t) = \underbrace{F_{\mathrm{GDP}}^{cap}(j, k, t)}_{\text{Global macro factor}} \cdot \underbrace{F_{pop}(x, y, k, t) \cdot \mathcal{L}_P(x, y)}_{\text{Local factor}}. \quad (1)$$

where $\mathcal{L}_P(x, y)$ is the data from Eberenz et al. (2020). The factor F^{cap}_{GDP} is the projected GDP per capita growth for each region:

$$F^{cap}_{\text{GDP}}(j, k, t) \quad = \quad \frac{\text{GDP}(j, k, t)/\text{GDP}(j, t = 2020)}{P(j, k, t)/P(j, t = 2020)} \tag{2}$$

where P is the total population of the region retrieved from SSP database (Riahi et al., 2017)[1]. Figure 3 displays the scenario-based projections of GDP and population in the five SSP, at the regional level by the IIASA model.

Figure 3: Regional F_{cap} factor variation in SSPs IIASA database

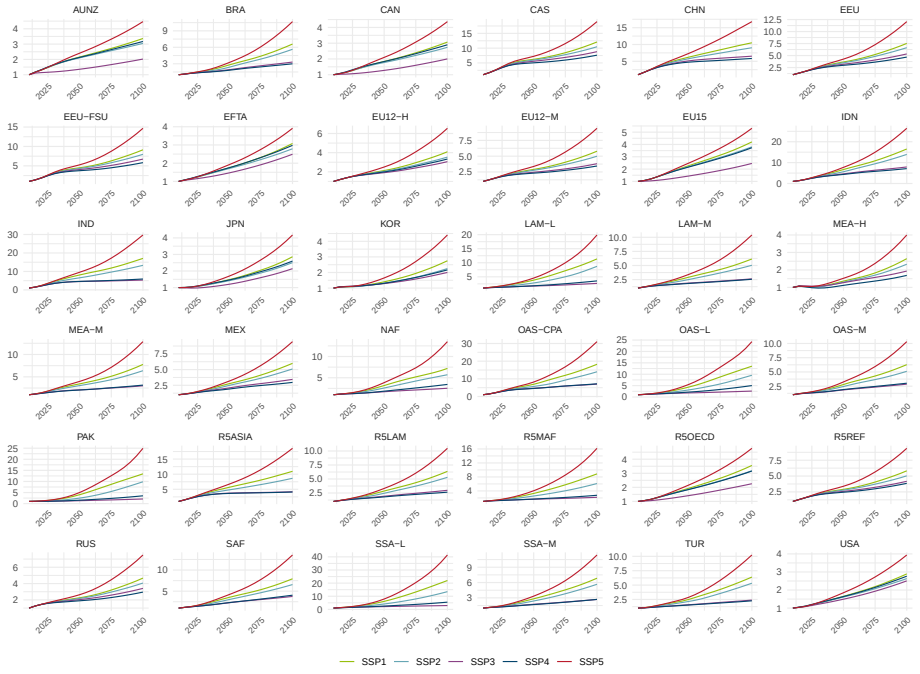

Source : https://tntcat.iiasa.ac.at/SspDb/.

The factor F_{pop} is defined as follows:

$$F_{pop}(x, y, k, t) \quad = \quad \frac{p(x, y, k, t)}{p(x, y, t = 2020)} \tag{3}$$

where $p(x, y, k, t)$ represents the local projections of population Jones and O'Neill (2020) illustrated Figure 4. We will detail this methodology in the manuscript.

[1] https://tntcat.iiasa.ac.at/SspDb/.

Figure 4: Variation of population exposure in 2100

(a) The middle road (SSP2)

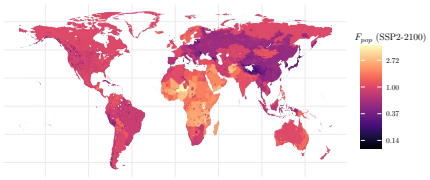

(b) The rocky road (SSP3)

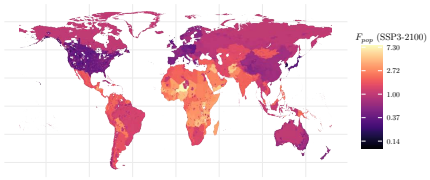

(c) Inequality (SSP4)

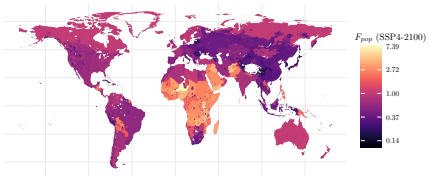

(d) Highway (SSP5)

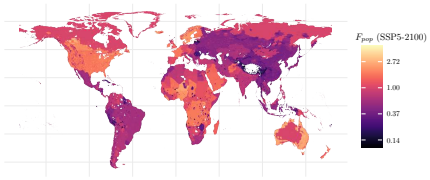

The scenario-based population grid generation is detailed by Jones and O'Neill (2020) with a last version downscaled at 1km following Gao (2020). This population grid is available every 10 years. We use the closest value in the definition of the exposure.

2 Technical comments

- Page 4, footnote 2: Please use the full reference for the Copernicus Climate data store (Hersbach et al., 2020)

- done

- Figures need to be larger to be legible.

- Figure 3: Recommend plotting each track with the same vertical scale (on the pressure and wind axes respectively) - i.e. use a scale of 0-75 m/s for wind speed and 880 - 1025 hPa for pressure on all panels. This will aid intercomparison of the time histories

- We will review all Figures in the next version

- Line 135: Please include an equation label

- done

- Page 7 - footnote: References to World Bank (2019b) and Credit Suisse Research Institute (2017) in the footnote of page 7 are not included in the bibliography.

- done

- Page 11: Footnote 13 should be in the body of the manuscript, as this is a key difference between James and Mason (2005) and the implementation in the current study. Following on from this, Tables A2, A4 and A6 reflect basin-wide fits, while the tracking method uses 5-by-5 degree grid. It may be more appropriate to provide maps of the relevant coefficients on the grids in the Appendix rather than the tables.

- done for the footnote and we replace table by relevant maps 5 to illustrate the specification.

Figure 5: Example of maps of coefficient and statistics

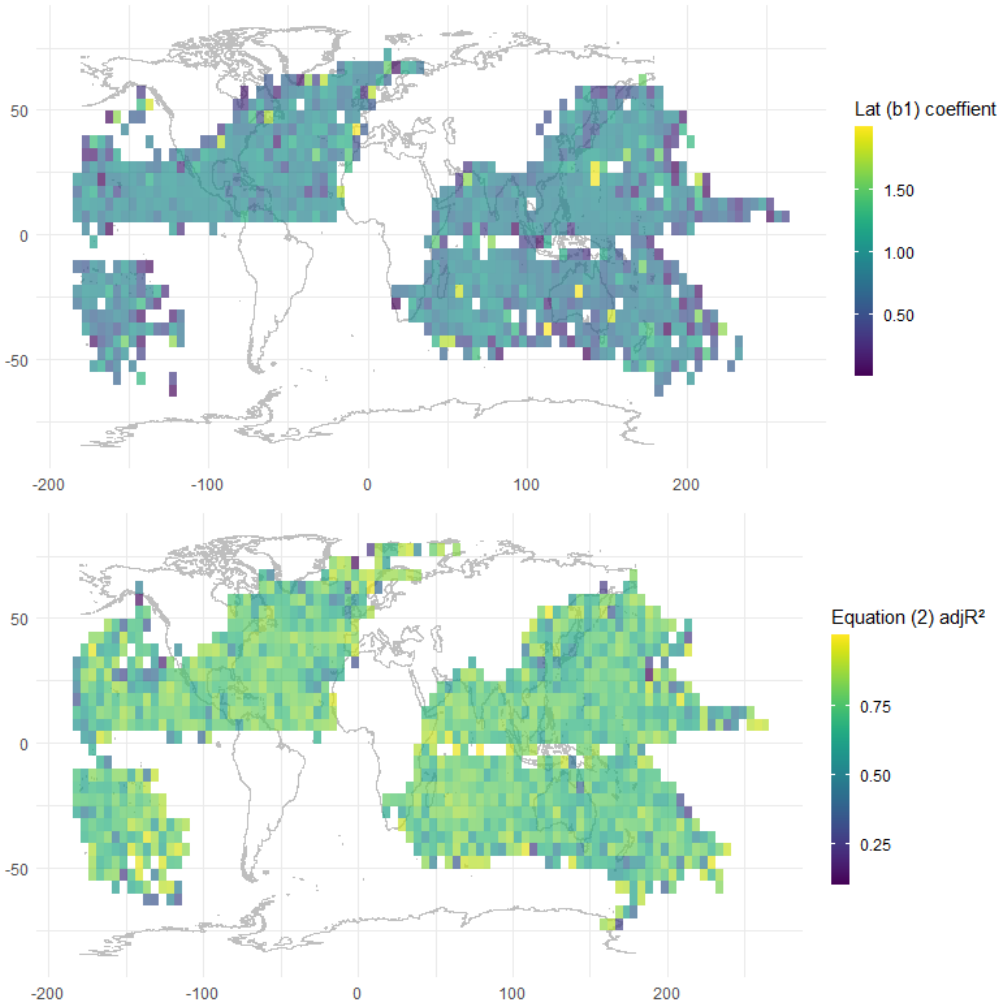

- Page 17, line 289: Does "This study" refer to the current manuscript, or to the previously referenced Unawa et al. (2000). Please clarify.

- done

- Page 20, line 333: Change "non-EOCD" to "non-OECD"

- Page 24, line 376: suggest changing "unbiased" to "bias-corrected"

- done

- Figure A8: Add units to the horizontal axes of the plot, or indicate what the values are in the caption. Ideally, each of the sub-plots should also use the same horizontal scale to aid comparison

References

Arthur, W. C. (2021). A statistical–parametric model of tropical cyclones for hazard assessment. *Natural Hazards and Earth System Sciences*, *21*(3), 893–916.

Bloemendaal, N., Haigh, I. D., de Moel, H., Muis, S., Haarsma, R. J., & Aerts, J. C. (2020). Generation of a global synthetic tropical cyclone hazard dataset using storm. *Scientific Data*, *7*(1), 1–12.

Bruyère, C., Holland, G., Prein, A., Done, J., Buckley, B., Chan, P., Leplastrier, M., & Dyer, A. (2019). Severe weather in a changing climate. *Insurance Australia Group and National Center for Atmospheric Research, November. https://www. iag. com. au/sites/default/files/documents/Severe-weather-in-a-changing-climate-report-011119. pdf*.

Chen, Y., Gao, S., Li, X., & Shen, X. (2021). Key environmental factors for rapid intensification of the south china sea tropical cyclones. *Frontiers in Earth Science*, *8*, 727.

Courtney, J. (2009). Adapting the knaff and zehr wind-pressure relationship for operational use in tropical cyclone warning centres. *Australian Meteorological and Oceanographic Journal*, *58*(3), 167.

Courtney, J., & Burton, A. (2018). Joint industry project for objective tropical cyclone reanalysis: Final report. *Bureau of Meteorology, 87pp*.

Courtney, J. B., Foley, G. R., van Burgel, J. L., Trewin, B., Burton, A. D., Callaghan, J., & Davidson, N. E. (2021). Revisions to the australian tropical cyclone best track database. *Journal of Southern Hemisphere Earth Systems Science*, *71*(2), 203–227.

Eberenz, S., Stocker, D., Röösli, T., & Bresch, D. N. (2020). Asset exposure data for global physical risk assessment. *Earth Syst*, *12*. https://doi.org/10.5194/essd-12-817-2020

Gao, J. (2020). Downscaling global spatial population projections from 1/8-degree to 1-km grid cells. *Technical Notes NCAR, National Center for Atmospheric Researcher, Boulder, CO., USA*. https://doi.org/10.7927/q7z9-9r69

Hall, T. M., & Jewson, S. (2007). Statistical modelling of north atlantic tropical cyclone tracks. *Tellus A: Dynamic Meteorology and Oceanography*, *59*(4), 486–498.

Harper, B. (2002). Tropical cyclone parameter estimation in the australian region. *Systems Engineering Australia Pty Ltd for Woodside Energy Ltd, Perth*, *83*.

Holland, G. J. (1997). The maximum potential intensity of tropical cyclones. *Journal of the atmospheric sciences*, *54*(21), 2519–2541.

Jones, B., & O'Neill, B. C. (2020). Global one-eighth degree population base year and projection grids based on the shared socioeconomic pathways. *Palisades*, (Revision 01).

Knutson, T., Camargo, S. J., Chan, J. C., Emanuel, K., Ho, C.-H., Kossin, J., Mohapatra, M., Satoh, M., Sugi, M., Walsh, K., et al. (2020). Tropical cyclones and climate change assessment: Part ii: Projected response to

anthropogenic warming. *Bulletin of the American Meteorological Society*, *101*(3), E303–E322.

Kossin, J. P. (2018). A global slowdown of tropical-cyclone translation speed. *Nature*, *558*(7708), 104–107.

Kossin, J. P., Emanuel, K. A., & Vecchi, G. A. (2014). The poleward migration of the location of tropical cyclone maximum intensity. *Nature*, *509*(7500), 349–352.

Lee, C.-Y., Tippett, M. K., Sobel, A. H., & Camargo, S. J. (2016). Rapid intensification and the bimodal distribution of tropical cyclone intensity. *Nature Communications*, *7*(1), 1–5.

O'Neill, B. C., Kriegler, E., Ebi, K. L., Kemp-Benedict, E., Riahi, K., Rothman, D. S., van Ruijven, B. J., van Vuuren, D. P., Birkmann, J., Kok, K., et al. (2017). The roads ahead: Narratives for shared socioeconomic pathways describing world futures in the 21st century. *Global environmental change*, *42*, 169–180.

O'Neill, B. C., Kriegler, E., Riahi, K., Ebi, K. L., Hallegatte, S., Carter, T. R., Mathur, R., & van Vuuren, D. P. (2014). A new scenario framework for climate change research: The concept of shared socioeconomic pathways. *Climatic change*, *122*(3), 387–400.

Riahi, K., van Vuuren, D. P., Kriegler, E., Edmonds, J., O'Neill, B. C., Fujimori, S., Bauer, N., Calvin, K., Dellink, R., Fricko, O., Lutz, W., Popp, A., Cuaresma, J. C., KC, S., Leimbach, M., Jiang, L., Kram, T., Rao, S., Emmerling, J., ... Tavoni, M. (2017). The shared socioeconomic pathways and their energy, land use, and greenhouse gas emissions implications: An overview. *Global Environmental Change*, *42*, 153–168. https://doi.org/10.1016/j.gloenvcha.2016.05.009